Pergamon

Geochimica et Cosmochimica Acta, Vol. 59, No. 20, pp. 4205–4218, 1995

0016-7037/95 $9.50 + .00

0016-7037(95)00288-X

Chemical mass balances in metalliferous deposits from the Atlantis II Deep, Red Sea

PIERRE ANSCHUTZ* and GÉRARD BLANC

Centre de Géochimie de la Surface, UPR CNRS n° 6251, Institut de Géologie, Université Louis Pasteur 1, rue Blessig, 67084 Strasbourg Cedex, France

(*Received March* 25, 1994; *accepted in revised form June* 16, 1995)

Abstract—In order to assess the quantitative distribution of mineral species within the sedimentary series of the Atlantis II Deep, we have examined the chemical composition, mineralogy, and physical properties of 120 sediment samples from two cores that sampled the entire sediment sequences in the West and South-West basins. Biostratigraphic correlations and chemical budget calculations indicate that the nonmetalliferous solid fractions (i.e., detrital and biogenic particles) in the older sedimentary unit (unit 1 in the West basin) represent 46% wt of the total, and that they were deposited between 23,000 and 15–12,000 years BP with a mass accumulation rate between 109 and 150 kg per thousand years per square metre. The muddy sediment in the upper part of the West basin core (units 2, 3, and 4) consists mainly of metalliferous particles which account for less than 15% wt of the mud, and yield a mass accumulation rate (130–162 kg/k.y./m^2) close to that of nonmetalliferous particles deposited simultaneously. Nonmetalliferous particles were probably the major source of Si and a significant source of Pb through dissolution in the brine system and diagenesis in the metalliferous mud. The metalliferous sediments in the upper unit of the South-West basin (unit U, 1100 cm) were deposited at the same time as those of the upper unit in the West basin (unit 4,335 cm). The calculated mass accumulation rate is about 700 kg/k.y./m^2 for unit U. The recent sediments of the South-West basin are more enriched in Zn and Cu, and more depleted in Mn relative to Fe than the contemporary sediments in the West basin, suggesting that the hydrothermal source has been in, or near, the South-West basin during the last 2,250 years. Assuming that a Salton Sea–like solution supplies all the Fe contained in the West basin metalliferous sedimentary pile, the mineralizing brine flowed at a minimum rate of 30 L/s. Except for the period of Mn-oxide deposition, the difference between the metal/Fe ratios in oxide-rich and sulphide-rich facies is attributed to changes in the chemical composition of the mineralizing fluid rather than to chemical processes acting in the brine system of the Atlantis II Deep.

1. INTRODUCTION

The Atlantis II Deep is the largest brine-filled closed basin located on the Red Sea axial rift zone (Fig. 1). The rift zone is covered or bordered by a thick Miocene evaporite sequence. These evaporites contribute to the formation of the dense NaCl-rich brines that accumulate in the depression. Previous studies have shown that about 5 km^3 of brines are stratified into two dense and convective layers of distinctly different temperature and chlorinity (Turner, 1969; Bäcker and Schoell, 1972; Voorhis and Dorson, 1975; Schoell, 1975; Schoell and Hartmann, 1973, 1978; Hartmann, 1980). A 10–30 m thick layer of metalliferous sediment occurs at the bottom of the brine pool, overlying tholeiitic basalts (Bäcker and Richter, 1973). The metalliferous sediments are fine-grained, delicately banded silicates, sulfides, oxides, and carbonates which have been accumulating for 25,000 years (Ku et al., 1969; Shanks and Bischoff, 1980). The Atlantis II Deep, presently covered by stratified brine, is limited by the 2000 m depth contour, and is divided into four subbasins called North (N), East (E), South-West (SW), and West (W). They are separated by bathymetric highs that do not extend above the top of the brine pool.

The processes involved in the precipitation of the Atlantis II Deep metalliferous sediments have been intensively investigated since 1965 (Miller et al., 1966; Degens and Ross, 1969; Hackett and Bischoff, 1973; Shanks and Bischoff, 1977, 1980; Danielsson et al., 1980; Pottorf and Barnes, 1983; Hartmann, 1985; Blanc, 1987; Zierenberg and Shanks, 1988). These studies yielded a great deal of information concerning the physical and chemical nature of metalliferous sediments, but little concerning sources, sinks, and fluxes of sedimentary material. The Atlantis II Deep is a dynamic system with mineral precipitation, occurring in multiple environments, all contributing to the deposition of metalliferous sediments. At the present, sulphides are precipitating in the reducing lower brine (Bäcker, 1976; Shanks and Bischoff, 1980; Hartmann, 1985), iron-oxides in the upper brine (Bischoff, 1969; Danielsson et al., 1980; Hartmann, 1985), manganese-oxides in the overlying transition zone (Danielsson et al., 1980; Hartmann, 1985), and authigenic silicates at the sediment-brine interface (Anschutz and Blanc, 1995). These mineralogical phases can be coprecipitated, and some of them have been redissolved during the settling out from the environment in which they precipitated. The composition of metalliferous sediments depends, among others, on the temperature and the composition of the inflowing brine, the volume of the brine pool, the surface area of the upper boundary of the lower brine pool, the temperature, the chemical composition, and the stability of the overlying brine layers. Temperature changes of the lower brine pool show that the hydrothermal activity has varied over small timescales (Ramboz and Danis, 1989; Blanc and Anschutz, 1995). Thus, one can only make rough estimates of the changes in the chemical composition and the flux of the hydrothermal fluid on the basis of the changes in the sediment

* *Present address:* INRS-Océanologie, 310 allée des Ursulines, Rimouski, Québec G5L 3A1, Canada.

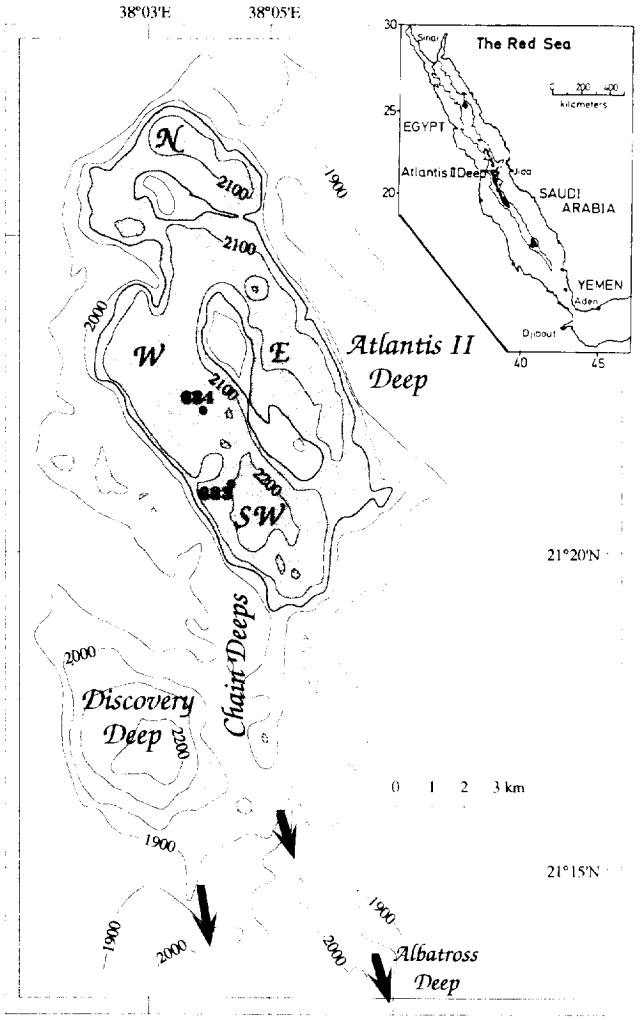

FIG. 1. Bathymetric map of the Atlantis II Deep area and location of Cores 683 and 684. SW, W, E, N: South-West, West, East, and North Basins. Contour lines have been traced from seabeam investigations (Pautot, 1983) and corrected with sound velocity calculations for Red Sea water. Corrections also have been made for the higher sound velocity in the brines. Grey areas correspond to the brine-filled deep. The 2000 m contour line corresponds approximately to the top of this area. The darkest area limited by the 2050 m line shows the extention of the Atlantis II Deep lower brine. Southwards arrows indicate the direction of the overspill of the dense brine pool, based on the present-day topography.

chemistry. However, whatever the chemical processes and the hydrodynamics were that lead to the formation of the sedimentary pile during the history of the Atlantis II Deep, the sediment was derived from chemical components that were supplied to the Atlantis II Deep system.

We report the results of a study of the chemistry, mineralogy, and physics of two cores that contain the entire sedimentary sequence of the W and SW basins. These data, in combination with estimated sedimentation rates, allow us to propose a chemical mass balance of the metalliferous sediments that takes into account the nonmetalliferous fluxes, i.e., biogenic and detrital phases. We also provide an estimate of the average discharge of inflowing mineralizing fluids and the changes that have occurred in their chemical composition in comparison with other hydrothermal systems. The purpose of this study is to evaluate the relative importance of the various sources that contributed to the sediment pile over the time span recorded by the stratigraphy.

2. MATERIAL AND METHODS

2.1. Material

Two cores were collected during the "Hydrotherm" cruise (May 1985) on the RV *Marion Dufresne* (Blanc et al., 1986; Blanc, 1987). Core 683 was collected in the SW basin at 2174 m and Core 684 in the W basin at 2110 m (Fig. 1). Both cores reached the basaltic substratum and recovered the entire sedimentary sequence present at these sites. Core 684 consists of millimetre to decimetre thick horizontal layers of an undisturbed sedimentary sequence. Disturbed layers, such as breccias or slumps were recognized in many Atlantis II cores (Bäcker and Richter, 1973). Allochthonous material does not occur in Core 684 nor in the upper part of Core 683. However, disturbances occur within the lower 2 m of the bottom part of Core 683. The destruction of the stratification in this layer could have been caused by a basaltic sill penetration and associated flows of hydrothermal brine, with subsequent conversion of iron oxides into magnetite (Zierenberg and Shanks, 1983). The silicates and the poorly crystallized Fe- and Si-bearing components in both cores were described by Badaut (1988) and Badaut et al. (1990).

A total of 120 samples, 3 to 10 cm thick, were taken from Cores 683 and 684 to define the mineralogical and chemical variability along the sedimentary sequences. Chemical and mineralogical analysis of dried and powdered marine sediments is complicated by the presence of salt from the interstitial brine, which is close to saturation with respect to halite (Anschutz, 1993). The samples were therefore washed with deionized water to remove the salts, dried at 40°C, and powdered. However, this treatment can induce the partial convertion of anhydrite into gypsum and bassanite. The mass gain due to calcium-sulphate hydration never exceeded 2% and was therefore not corrected for in the chemical analyses. Some calcium-sulphate may also dissolve, and Ca, Sr, and S concentrations may potentially be slightly affected by washing. Raising the pH of the deionized water is required to avoid losing a significant component of adsorbed cations. We used slightly acidic deionized water, with pH similar to that of the present-day brine, to wash the samples.

2.2. Chemical Analysis

Samples for the analysis of the major element composition were prepared by fusing 100 mg of powdered, dried, and salt-free sediments with 750 mg of lithium tetraborate in a glassy graphite melting pot at 1000°C followed by dissolution in a glycerin-hydrochloric acid solvent (Samuel et al., 1985). The alkaline fusion resulted in complete dissolution of the major elements, but the volatile elements Pb and Zn were partially lost. A tri-acid attack ($HCl + HF + HClO_4$ at 120°C in Teflon crucibles during 10 days) of 1g powdered sediment was used to determine of Zn and Pb. Iron, Mn, Si, Al, Ca, Mg, Zn, Pb, Cu, Ti, and Zr were determined by Inductively Coupled Plasma–Atomic Emission Spectroscopy (ICP–AES). The precision is 2–5% for the major elements and 10% for Pb and Zr. The accuracy, determined with the aid of marine international standards, was within 5%. Sodium and potassium were determined with flame emission spectrometry with Li as an internal standard. Sulfur and carbon were quantified by infrared absorption photometry using a Leco 125. The fraction of S in anhydrite or in sulphide minerals was deduced from the Ca, Zn, Cu, and Fe contents, using the normative method described below. Because the organic carbon content is below 0.2% throughout these sediments (Blanc et al., 1990), the C content is assumed to be present exclusively as carbonate. The precision was better than 10% for Na, K, C, and S. The results are reported in Tables 1 and 2.

2.3. Mineralogy

The mineralogy was determined by X-ray diffraction (XRD) analysis of powdered sediment with a Philips PW 1710 diffractometer

Table 1. Chemical composition in grams/kilograms (g/kg) of dry and salt-free sediments sampled in Core 683 (SW basin). (-) : not determined.

	Depth (cm)	Fe	Mn	Si	Al	Ca	Mg	Zn	Cu	S	C	Na	K	Sr	Pb	Zr	Ti
	5	245	0.9	88	10.4	14.0	4.5	90.0	10.50	67.7	7.3	4.5	1.3	0.14	2.00	-	-
	50	291	0.7	108	11.6	12.2	5.2	97.2	11.76	89.6	8.6	3.3	2.7	0.10	2.10	0.034	0.6
	91	325	2.2	98	6.9	20.0	5.8	54.9	7.79	43.8	8.2	4.7	3.5	0.20	1.40	0.022	0.3
	110	275	2.5	97	7.8	20.0	5.0	58.0	7.90	41.3	6.4	5.6	1.1	0.17	1.36	-	-
	155	276	0.9	88	7.4	10.0	5.5	113.4	9.26	65.9	4.7	8.1	3.3	0.09	1.07	0.014	0.3
	185	296	0.6	98	7.4	34.3	3.9	43.7	2.56	79.5	8.8	1.7	2.2	0.14	1.04	0.020	-
	200	355	7.2	108	7.4	20.0	6.1	36.5	7.68	52.0	10.2	2.6	3.7	-	0.65	-	0.6
	224	299	2.9	109	6.9	29.3	6.5	34.5	6.16	47.6	6.3	5.9	5.0	0.40	1.24	0.027	0.36
	275	300	4.1	81	4.2	25.5	3.4	18.0	4.60	41.5	4.0	6.2	1.0	0.66	0.53	0.026	-
	315	283	1.3	89	8.5	13.5	4.5	52.0	6.90	42.8	3.6	6.5	1.5	0.17	1.08	-	-
	350	416	4.8	93	5.8	10.0	3.8	46.0	7.82	54.5	9.7	1.9	1.2	0.09	0.68	0.027	0.42
	365	367	1.9	88	6.4	12.1	4.1	29.4	6.90	47.9	3.9	6.2	3.0	-	1.71	-	0.42
	420	310	1.5	84	5.6	10.0	3.4	54.0	7.10	45.4	3.8	5.4	1.0	0.12	1.01	-	-
	456	357	1.6	83	6.0	13.2	3.8	36.2	6.85	56.8	4.2	3.2	2.7	0.16	1.98	0.018	0.42
	490	309	12.0	136	8.5	22.2	7.7	33.6	4.68	29.6	14.1	3.9	5.0	0.18	0.78	0.029	0.6
	525	303	0.9	76	5.8	14.1	2.8	74.0	9.70	62.4	3.3	3.8	0.9	0.22	1.84	0.029	-
U	556	131	1.7	45	3.2	142.2	2.4	30.3	3.41	135.9	9.3	0.7	1.0	0.52	0.62	0.011	-
N	603	244	6.0	85	6.9	74.3	5.7	38.1	5.29	83.9	9.2	2.5	3.5	0.88	1.58	0.032	0.48
I	662	254	0.8	88	5.0	13.4	4.5	68.0	7.70	39.0	4.2	10.0	1.4	0.20	1.20	0.024	-
T	696	316	2.3	107	9.2	17.4	6.4	126.3	11.56	76.0	8.2	3.1	4.7	0.37	3.12	0.029	0.54
	728	263	3.9	77	5.8	10.5	4.0	68.0	10.10	64.8	5.4	6.1	1.5	0.58	3.40	-	-
	782	344	9.1	87	2.1	14.3	6.0	40.4	5.15	63.0	11.3	2.4	3.3	0.25	1.19	0.022	0.18
U	828	330	4.3	84	6.4	13.5	13.7	36.0	7.90	40.8	7.8	4.9	1.0	0.14	0.80	-	-
	889	219	3.5	106	10.1	52.9	10.6	52.8	4.34	100.9	10.0	3.3	4.0	0.13	1.53	0.017	-
	918	227	4.1	101	7.8	22.5	7.5	66.0	7.10	69.8	10.3	5.3	3.3	0.10	1.50	-	-
	958	287	2.8	112	9.5	34.3	6.0	77.0	8.97	67.8	9.1	2.2	4.8	-	0.85	-	0.48
	981	243	0.8	83	6.4	49.3	5.0	91.4	3.30	120.1	6.3	0.9	2.5	0.12	1.39	0.014	-
	989	228	3.1	93	6.9	57.9	7.4	72.9	2.68	93.6	10.3	0.9	3.2	0.16	1.17	0.016	-
	997	224	4.6	78	8.5	3.8	9.7	32.0	6.86	97.5	17.9	1.4	2.7	0.14	0.43	0.014	-
	1020	241	1.9	124	7.4	42.2	7.5	92.7	7.32	90.9	4.9	1.9	3.1	0.18	0.80	0.024	0.3
	1033	211	8.8	107	7.4	32.9	9.4	72.7	2.38	69.8	16.0	2.7	2.8	0.14	1.46	0.018	-
	1048	174	12.4	93	8.9	15.0	7.5	112.5	11.70	110.9	29.7	5.0	1.8	0.15	2.05	0.020	-
	1067	206	3.3	121	7.4	24.3	14.4	61.8	2.52	107.1	15.1	4.5	1.5	0.10	1.65	0.012	-
	1077	173	2.2	110	8.5	51.5	13.9	53.0	1.18	116.2	8.7	0.6	1.3	0.10	2.03	0.013	-
	1085	85	0.9	101	11.1	84.6	50.7	95.0	1.42	198.6	9.8	4.1	2.3	0.12	2.26	0.014	-
	1090	90	0.5	99	12.7	54.9	2.5	237.1	15.50	235.0	4.1	9.7	4.0	0.23	3.11	0.016	0.36
	1091	48	0.7	60	6.4	134.4	1.6	96.7	4.33	206.5	4.9	5.0	2.1	0.48	0.58	0.009	-
	1102	21	2.6	35	1.1	234.4	0.5	11.7	0.91	155.7	4.2	0.6	0.4	1.42	0.15	0.003	-
	1113	69	3.5	52	2.1	146.5	2.0	64.5	4.04	123.1	5.9	2.2	0.7	1.03	0.26	0.006	-
	1118	129	3.6	115	3.7	87.2	3.7	48.1	1.19	186.7	12.4	0.6	0.4	0.33	0.13	0.010	-
	1128	28	2.5	13	0.7	230.0	0.8	9.0	1.90	226.8	2.9	0.6	0.6	1.25	0.11	0.009	-
	1169	43	1.2	13	1.1	273.7	1.9	5.1	1.21	259.8	4.4	1.0	0.4	0.89	0.14	0.004	-
	1198	400	2.4	36	3.6	64.0	3.6	1.4	2.50	51.0	5.2	1.7	0.5	0.84	0.06	0.018	-
	1240	144	7.4	17	1.5	198.7	3.4	0.1	0.68	155.6	9.3	1.2	0.4	0.77	0.10	0.016	0.3
	1260	195	1.6	34	1.9	168.7	25.3	1.6	0.53	121.9	2.0	1.0	0.4	0.49	0.16	0.019	0.18
U	1320	69	3.4	11	1.1	290.9	3.3	0.2	0.03	163.3	23.6	0.7	0.4	0.88	0.11	0.003	-
N	1350	156	2.7	36	2.7	188.7	5.9	0.1	0.56	114.5	13.4	1.0	0.4	0.45	0.63	0.019	0.42
I	1389	171	1.1	29	2.1	205.1	2.5	0.2	0.07	169.2	3.9	1.0	0.4	0.70	0.15	0.008	-
T	1428	418	2.7	61	2.6	33.5	53.2	0.3	0.04	22.9	0.4	0.6	0.5	0.09	0.04	0.028	-
	1465	248	2.3	129	27.5	72.9	62.7	0.1	0.03	32.6	0.8	7.6	0.4	0.16	0.33	0.031	2.94
	1485	282	1.2	63	3.7	95.1	55.3	0.1	0.02	71.1	1.2	1.9	0.4	0.23	0.12	0.002	-
L	1508	253	1.4	45	2.8	103.0	38.0	0.2	0.03	72.4	0.3	4.3	0.5	0.44	0.04	-	-
	1560	304	1.4	51	3.2	124.4	46.2	0.1	0.18	57.5	0.3	1.0	0.4	0.41	0.33	0.021	0.18
	1599	138	1.1	33	1.6	208.0	29.9	0.1	0.04	81.6	0.6	0.7	0.4	0.78	0.12	0.006	-

using CuKα X-Radiation. The semiquantitative X-ray method of Hooton and Giorgetta (1977), which relies on empirically derived intensivity factors for the various minerals, was used for quantitative mineralogy by reference to an internal standard. The precision was improved by using the chemical data via a normative procedure. In this procedure each element in a given sample is assigned to a succession of minerals that have been determined by XRD. For example, in a sample which contains pyrite, sphalerite, and chalcopyrite, we assign all Zn to sphalerite, and all Cu to chalcopyrite. This assumption is consistent with the low Zn and Cu contents of clays, hydroxides, and carbonates from the Atlantis II Deep (Brockamp et al., 1978; Missack et al., 1989). The pyrite content is obtained from the remaining S. If the same sample contains anhydrite, but no calcite, the Ca content is assigned to the excess S prior to calculating the amount of pyrite. Because of the assumption of ideal mineral stoichiometry and because of the variable crystallinity of some of the minerals, the precision of the mineralogical composition determined by the normative procedure may sometimes be low. The distribution of cations in solid-solution carbonates was estimated by the position of the (104) diffraction peak (Goldsmith and Graf, 1958). Elements in excess after partitioning into identified minerals (mainly Fe and Si) were attributed to clays and silico-ferric phases, which are ubiquitous but cannot be determined precisely on powdered sediment by XRD. The Fe/Si ratios deduced from excess Fe and Si were always similar to the stoichiometric Fe/Si ratios of clay minerals determined on Cores 683 and 684 by Badaut (1988). Simultaneous use of the semiquantitative X-ray method and the chemical composition permits the proportion of minerals to be determined with a precision better than 20%, which is sufficient for our purpose. Additionally, the granulometric fraction greater than 63 μm was extracted for microscopic observations to recognize and quantify biogenic particles and coarse detrital particles. The results of the micropalaeontological study are reported by Anschutz and Blanc (1993a).

2.4. Porosity and Density

The proportions of water, salt dissolved in the interstitial water, and salt-free sediment in seventy-three subsamples

Table 2. Chemical composition in grams/kilograms (g/kg) of dry and salt-free sediments sampled in Core 684 (W basin). (-) : not determined.

	Depth (cm)	Fe	Mn	Si	Al	Ca	Mg	Zn	Cu	S	C	Na	K	Sr	Pb	Zr	Ti
	5	336	5.9	100	7.4	25.7	6.0	23.2	4.04	29.4	16.1	2.8	4.3	0.45	1.01	0.030	0.01
	35	258	2.0	125	5.5	14.5	6.0	28.0	4.60	18.3	10.3	10.0	3.9	0.38	0.64	-	-
	100	368	3.6	126	7.9	12.9	5.6	30.0	7.59	21.3	11.2	2.1	4.9	0.54	0.78	0.039	0.66
U	140	250	5.8	131	10.6	43.6	10.7	38.9	6.82	24.6	15.9	7.0	7.1	0.22	0.30	-	0.84
N	170	284	2.8	151	9.0	40.0	9.5	35.5	4.97	17.7	13.9	7.8	6.2	0.32	0.68	0.041	0.6
I	190	192	7.6	120	11.6	41.5	7.6	54.0	6.20	51.0	13.7	12.6	3.3	0.25	1.13	-	0.84
T	215	290	2.6	128	10.1	20.0	6.7	31.4	1.61	51.3	14.2	1.2	7.6	0.12	1.26	0.023	-
	240	259	10.0	146	12.2	30.0	9.0	61.4	6.60	40.6	15.1	5.1	6.7	0.19	0.83	0.049	0.66
4	260	340	0.6	110	7.9	10.7	4.5	81.0	10.79	67.6	4.3	7.1	2.1	0.12	2.07	0.020	0.54
	271	261	0.8	173	13.3	6.9	9.4	102.6	10.15	129.0	0.7	5.3	6.8	0.14	0.01	0.032	0.54
	312	165	4.4	172	13.1	15.1	4.1	138.1	15.71	165.0	11.2	7.6	4.8	0.82	1.96	0.028	0.54
	318	238	39.6	94	5.9	8.4	5.5	36.0	10.30	105.3	52.9	5.1	1.2	0.83	0.57	-	-
	330	292	36.0	69	6.4	19.3	4.3	4.6	2.42	57.8	52.8	2.4	2.0	1.33	0.56	0.021	-
	335	292	54.4	55	6.9	13.6	4.3	8.7	1.48	31.5	68.0	2.8	2.0	1.88	0.49	0.020	-
	340	459	33.5	34	4.2	12.9	2.4	5.4	0.72	6.3	28.3	1.5	1.3	0.79	0.65	0.028	0.48
	381	525	56.8	23	1.6	3.6	1.6	7.3	1.17	2.8	12.2	1.1	0.6	0.05	0.63	0.023	0.24
	415	485	32.3	23	1.4	2.0	1.1	5.0	0.58	4.1	5.8	2.7	0.5	0.06	0.11	0.033	-
	442	120	313.3	10	2.1	7.9	9.6	2.8	1.25	2.8	3.6	1.1	4.5	1.31	0.10	0.021	0.12
	480	108	377.6	10	1.4	5.0	10.9	2.1	0.76	4.0	2.5	7.2	2.3	0.79	0.15	0.023	-
	502	403	186.6	20	1.7	2.1	2.9	4.9	0.95	2.2	1.8	2.6	1.0	0.29	0.63	0.019	0.12
	550	262	265.0	14	1.9	1.2	2.4	2.6	1.30	1.9	0.9	1.1	0.7	0.13	0.13	-	-
	590	516	52.0	29	0.1	7.9	3.0	3.5	1.12	3.0	6.4	1.6	0.9	0.07	0.35	0.027	0.12
	600	484	49.4	38	2.7	15.0	3.7	3.3	0.94	2.8	10.3	1.3	1.3	0.07	0.10	0.028	0.24
U	611	452	64.0	29	2.7	5.7	2.2	5.9	0.92	4.2	13.2	0.4	0.4	0.07	0.09	0.021	-
N	630	506	20.7	48	2.7	10.7	3.7	6.8	0.92	1.8	13.9	2.5	1.1	0.10	0.70	0.023	0.36
I	650	432	41.6	40	1.7	6.5	2.2	1.6	1.10	2.3	6.4	3.0	0.6	0.14	0.14	0.033	-
T	690	425	33.6	51	2.7	63.6	3.9	4.5	1.72	2.4	32.2	1.9	1.2	0.13	0.75	0.018	0.18
	717	471	8.6	96	4.8	7.2	4.0	2.2	5.06	3.2	10.5	6.3	3.3	0.17	0.32	-	0.42
	745	365	31.8	143	3.7	8.6	7.3	5.2	2.76	4.5	14.9	5.7	7.8	0.16	0.10	0.025	0.3
3	778	376	24.7	85	4.8	15.0	7.0	3.7	3.54	4.4	30.5	5.0	2.3	0.47	0.37	0.023	-
	792	406	8.0	126	2.7	6.4	5.7	2.4	1.39	2.9	9.0	7.6	5.0	0.14	0.67	0.029	0.3
	821	412	23.2	89	4.8	17.9	7.2	5.9	1.14	2.2	30.4	4.5	2.7	0.19	0.85	0.025	0.54
	828	364	24.0	93	4.2	21.4	6.8	8.2	1.54	6.3	24.9	4.0	2.0	0.17	0.85	0.019	-
	848	285	65.0	29	4.7	9.5	4.5	68.0	7.70	97.2	27.3	1.3	1.0	0.48	3.70	-	-
	876	222	303.9	23	2.7	5.7	6.7	5.0	0.68	2.1	5.5	6.7	2.8	0.61	2.20	0.018	0.42
	901	97	359.1	16	2.3	3.5	5.5	2.1	0.63	2.4	1.6	3.8	1.4	0.45	0.48	-	0.36
	933	292	226.9	28	2.7	5.0	4.7	1.8	0.90	2.0	0.1	5.6	2.7	0.39	0.52	0.031	0.18
	950	229	268.7	25	3.2	5.7	6.7	2.4	0.50	0.2	3.5	6.8	3.2	0.62	0.23	0.020	-
	956	425	102.0	43	3.7	12.2	4.0	3.2	0.51	1.6	11.2	2.5	2.7	0.14	0.75	0.021	0.48
	975	519	25.9	45	3.7	11.4	2.7	2.2	0.31	2.9	7.3	3.6	2.1	0.07	0.10	-	0.36
	993	300	5.9	192	5.3	13.6	9.2	9.9	1.18	3.0	7.4	2.7	9.3	0.10	0.24	0.020	-
	1000	171	44.0	103	16.0	62.2	11.5	20.5	11.25	46.6	60.0	4.3	7.1	0.16	0.90	0.044	1.26
	1002	26	7.3	133	19.1	72.2	8.3	76.8	2.49	114.5	41.9	3.5	7.6	0.26	2.72	0.044	-
U	1026	113	5.2	128	10.7	5.5	3.4	141.5	25.50	190.3	16.7	5.3	1.5	0.15	2.25	0.023	0.36
N	1051	113	21.8	81	14.8	43.6	9.2	102.7	2.41	133.7	41.5	4.5	3.6	0.10	0.77	0.023	-
I	1062	194	20.8	141	15.4	17.8	6.8	51.2	17.55	167.8	35.0	6.3	4.2	0.10	2.10	0.028	0.96
T	1081	285	26.8	151	1.6	17.5	7.0	1.0	3.30	28.5	13.6	7.0	1.5	0.07	0.32	0.031	-
	1100	254	1.6	217	2.1	10.7	7.7	4.0	4.86	24.8	6.2	14.5	12.6	0.09	0.47	0.015	-
	1108	71	1.8	166	4.2	68.6	1.9	52.5	6.97	161.9	13.3	2.4	1.7	0.45	1.54	0.009	-
2	1119	200	2.9	177	9.8	15.0	6.0	14.7	25.42	145.4	11.5	7.3	8.6	0.05	2.48	0.021	0.6
	1123	201	34.3	81	7.9	38.6	7.7	9.7	1.35	85.7	62.1	4.0	3.2	0.07	1.16	0.016	-
	1131	61	9.9	108	13.2	32.9	6.0	98.5	2.29	155.7	32.1	7.4	4.2	0.11	1.91	0.018	-
	1136	78	5.9	83	13.0	50.0	5.0	165.0	25.50	171.0	13.8	3.1	2.0	0.72	1.95	0.030	0.48
	1146	171	37.0	65	10.6	20.7	13.7	51.7	0.06	119.6	75.3	3.6	3.2	0.10	0.97	0.025	-
	1150	112	8.9	71	14.3	130.8	5.8	9.8	3.64	157.9	20.4	2.8	3.7	0.48	0.76	0.025	-
	1155	159	45.6	25	6.9	115.8	11.4	1.4	1.55	99.8	56.9	5.6	1.7	1.08	0.16	0.018	-
	1159	405	38.3	32	3.7	17.2	4.8	7.0	1.15	11.2	31.5	12.6	1.3	0.52	0.11	0.023	-
	1162	469	53.3	50	3.2	7.2	3.3	5.2	0.18	2.1	13.2	1.6	2.1	0.02	0.10	0.022	0.36
	1176	100	108.1	48	13.2	125.8	21.4	5.4	0.54	39.1	85.5	2.6	4.0	0.29	0.27	0.053	1.02
U	1194	115	8.8	189	49.7	32.2	17.3	16.8	1.36	113.0	21.9	10.8	12.5	0.22	0.10	0.229	5.4
N	1209	494	8.9	52	8.5	15.0	12.4	4.6	0.23	4.8	23.0	3.6	2.9	0.04	0.10	0.050	0.96
I	1229	490	4.0	19	2.4	4.5	4.5	0.9	0.07	2.7	11.9	3.1	0.8	0.02	0.05	0.032	-
T	1244	88	5.3	166	50.2	59.3	17.1	6.1	0.42	66.8	35.4	10.5	11.6	0.33	0.30	0.128	4.38
	1266	98	1.9	186	33.6	54.0	14.0	8.0	0.45	107.4	29.4	3.9	4.2	0.23	0.11	0.129	-
	1293	416	5.0	37	6.9	36.5	13.5	3.8	0.46	2.4	44.0	3.4	1.8	0.17	-	0.032	-
1	1295	313	11.2	14	4.2	71.5	31.2	4.5	0.20	2.5	96.2	3.9	1.3	0.26	0.09	0.021	-
	1300	90	4.6	106	27.6	126.3	16.3	1.0	1.00	53.0	54.9	3.8	3.7	0.50	0.08	0.154	-
	1326	32	4.4	96	27.6	208.6	22.5	0.3	0.07	3.5	70.2	3.2	4.0	0.74	0.05	0.112	-
	1368	52	7.8	89	25.4	211.6	23.9	0.1	0.06	2.8	78.1	5.0	8.4	0.60	0.35	0.082	2.04

were estimated by successive weighing of bulk mud, dried sediment, and washed and redried sediment kept in the same container (Blanc et al., 1986). The amount of crystalline halite in the sediment was insignificant (Anschutz and Blanc, 1993b). The density of bulk muds was estimated from the density of each phase, i.e., 1.2 g/cm^3 for the interstitial brines (IB), which corresponds to water + salt, and 3 g/cm^3 for the solid fraction (SF). Density (ρ) is calculated as $\rho = [(IB)/1.2 + (SF)/3]^{-1}$.

3. RESULTS

3.1. Mineralogy

The high depth resolution of the subsampling and the normative procedure for quantifying the distribution of major minerals allow us to define precisely the lithological units. The resulting definition is more detailed than that proposed

by Bäcker and Richter (1973), which was based on multiple cores but with lower stratigraphic resolution (Fig. 2). The new lithologic description presented in this paper can nevertheless be compared readily to that of Bäcker and Richter (1973). Based on Core 684, the thicknesses of DOP (Unit 1) facies, SU1 (Unit 2), and SU2 (part of Unit 4) sulphide-bearing facies are 2.3 m, 1.55 m, and 1.80 m, respectively. These are very close to the average thicknesses of these facies (2.35 m, 1.30 m, and 1.60 m) calculated from several hundred cores collected in the W, E, and N basins (Urvois, 1988). The thickness of the CO (Unit 3) facies of Core 684 is 6.65 m, which is greater than the average for the Atlantis II Deep (i.e., 2.35 m; Urvois, 1988). However, the thickness of this facies is typical of the W basin. Core 684 therefore is representative of the entire sedimentary sequence of the Atlantis II Deep. Because the complete sedimentary series has rarely been recovered in the SW basin, average thicknesses of lithologic units could not be estimated in this basin (Urvois, 1988). However, the complete sedimentary series recovered in Core 683 is useful for studying the hydrothermal history of the SW basin.

3.1.1. Core 684

Core 684 from the W basin is divided into four main units in addition to the basalt which was recovered at the base of this core. Unit 1 (bottom to 1155 cm) is mainly detrital and biogenic material enriched in foraminifera, radiolaria, and

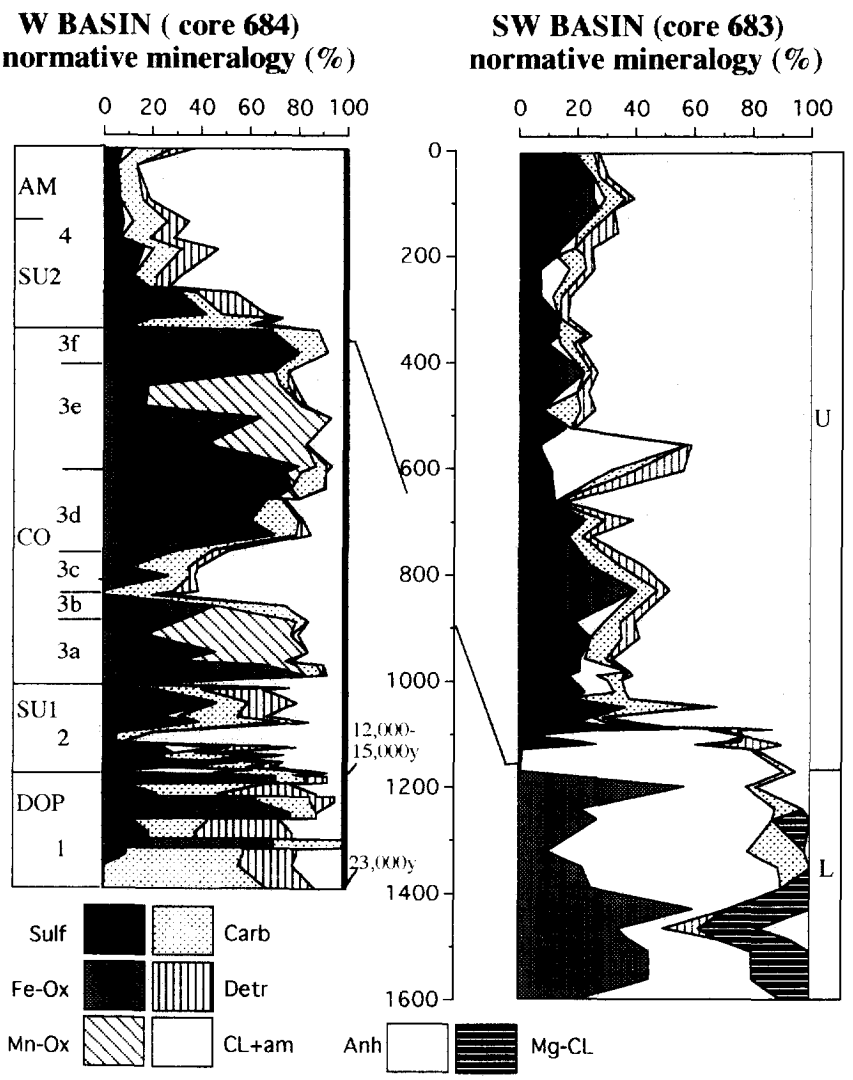

FIG. 2. Distribution of minerals vs. depth in Cores 683 and 684, expressed as weight percent of dry and salt free sediments. The ages (Core 684) were deduced from intercore correlation within the Red Sea using absolute abundance patterns of planktonic fauna. Lithological units defined in this study are caled 1, 2, 3, and 4 (Core 684) and U and L (Core 683). Corresponding facies proposed by Bäcker and Richter (1973) are shown for Core 684: detrital-oxide-pyrite (DOP), lower sulfide (SU1), central oxide (CO), upper sulfide (SU2), and amorphous-silicate (AM). Sulf: Sulphide minerals; Fe-Ox: iron oxide and oxyhydroxide; Mn-Ox: manganese oxide and oxyhydroxide; Anh: Anhydrite; Carb: Carbonates; Detr: Detrital silicates; CL + am: Clay minerals and amorphous Fe- and Si-compounds; Mg-CL: Magnesian phyllosilicates.

pteropod fragments. This sediment contains mixed Mn, Fe, Mg, and Ca carbonates, including ankerite, kutnahorite, dolomite, and siderite. The nonmetalliferous sediments are accompanied by pyrite, which presumably originates from the reaction between iron oxides and sulphide produced by bacterial sulphate reduction during early diagenesis (Shanks and Bischoff, 1980). Within unit 1, three stratified intercalations of goethite or lepidocrocite mixed with siderite are recognized.

Unit 2 is predominantly characterized by sulphide minerals. The S, Zn, Cu, and Fe contents indicate that the cumulative content of sphalerite, pyrite, and chalcopyrite is as high as 50%. The distribution of the three mineral species is not uniform. Two sulphidic layers occur between 1150 and 1100 cm and between 1066 and 1000 cm. These layers are separated by a thin layer of clay-rich sediment. Anhydrite is common at the bottom of unit 2. Carbonates in this unit are siderites that contain $MnCO_3$ in solid solution. Detrital silicates, mostly quartz and feldspar, and biogenic amorphous silica (diatoms and radiolaria), can comprise more than 20% of the sediment, estimated by observations under the binocular, but very few carbonaceous tests were found. The top of unit 2 is marked by a manganosiderite and calcite-rich layer.

Unit 3 is characterized by the predominance of iron and manganese oxides and oxyhydroxides. Goethite, hematite, manganite, groutite, and todorokite are the main mineral species with variable proportions throughout the unit. Subunit 3a (1000–875 cm) contains mostly goethite and manganite, accounting for 80% of the total. The content of manganite increases from 14% at the bottom to 60% at the top of this subunit. Unit 3b (875–835 cm) is a thin sulphidic subunit, containing manganosiderite but no Mn^{3+} or Mn^{4+} minerals. Hematite also occurs in this unit. Unit 3b is overlain by carbonate and iron silicate rich layers (unit 3c). The sediment from 750 to 600 cm (unit 3d) consists essentially of goethite (60–80%) and Ca, Fe, and Mn carbonates (6 to 20%). From 600–415 cm (unit 3e), the goethite becomes enriched in Mn as seen by the shift of the XRD peaks toward the groutite peak (Stiers and Schwertmann, 1985) and by the increase of the total Mn content. At shallower depth, the separate phases groutite and goethite occur, followed upward by manganite and todorokite. The core section from 415–335 cm (unit 3f) contains mostly goethite (50–70%) with minor amounts of hematite (10–20%), manganosiderite, and no calcite. The uppermost samples of this unit contain 3% anhydrite.

Unit 4 (335 cm to top of the core) is characterized by sulphides, clays, and poorly crystallized material which is considered to be Fe- and Si-bearing. The base of unit 4 is composed of manganeous siderite (50%), sulphide (16%), and calcium sulphate (3%), followed upwards by a ZnS-rich interval. The amount of ZnS decreases regularly upwards from 20% to 4% of the solid fraction, as we notice from the decrease in the Zn and S contents. The pyrite and chalcopyrite contents decrease in the same way as ZnS. At the top of the core (140–0 cm) the sulphides are X-ray amorphous and are therefore most likely to be iron monosulphides (Pottorf and Barnes, 1983; Zhabina and Sokolov, 1982; Brockamp et al., 1978). Samples of unit 4 contain up to 5% anhydrite. In this unit, Fe-Mn and Ca carbonates range from 3 to 15%. The Fe- and Si-bearing poorly crystallized portion comprises up to 85% of the solid fraction.

3.1.2. Core 683

Two major units were defined in the SW basin. The lower unit (unit L) consists of anhydrite (12 to 70%), talc, and serpentine (up to 28%) and iron oxides (20 to 60%). It can be divided into two different subzones: a magnetite-rich facies (bottom to 1365 cm) in which talc is a major component but with coarse basaltic fragments at 1465 cm, and a hematite-rich facies (1365 to 1180 cm) in which the anhydrite content is maximal. The hematite-rich facies contains carbonates (<11%).

The upper unit (unit U) is characterized by the presence of sulphides and abundant clay and Fe- and Si-bearing compounds. The lower part from 1180 to 1100 cm has a low sulphide content (<2%), predominantly ZnS, and is essentially composed of anhydrite (78 to 90%). At 1090 cm, sulphides become important and reach the highest value in either core (55%). The anhydrite content decreases significantly. The upper 10 m of the core has a relatively constant sulphide content (7 to 20%) except at 700 cm, 155 cm, and in the upper fifty cm, where the ZnS content is higher (from 19 to 25% of total sulphide minerals). Iron oxides and anhydrite appear sporadically in the upper part of unit U.

3.2. Physical Properties

In the uppermost 10 m of Core 683, the solids content is extremely low (from 5 to 12%) and therefore the density of the mud is close to the density of the brine. The porosity decreases abruptly at the bottom of unit U and the solid fraction increases to 58%. The solid content at the top of Core 684 (units 4 and 3) is similar to unit U of Core 683. The solids content increases rapidly in unit 2 and reaches a constant value of 46% in unit 1. The calculated densities are given in Table 3, and agree with direct density measurements via gamma densitometry on other cores from Atlantis II Deep (Thisse, 1982). For a box of 1 m^2 cross-section an height corresponding to the series of units 2, 3, and 4, the mass of the solid fraction is 1943 kg (Table 3). Because of the porosity variation, the mass of the salt-free dry sediment in the nonmetalliferous layer of unit 1 (called "non-met" in Table 3) corresponds to 32% of the total mass of the solid fraction of Core 684, whereas the thickness of this layer is only 11% of the total.

3.3. Geochemistry

The elementary composition of the sediment is plotted in Figs. 3 and 4. All the samples contain high concentrations of Fe (90 to 525 g/kg), except those enriched in detrital minerals and anhydrite. The Fe derives from iron-oxides or oxihydroxides, clays, and poorly crystallized Fe- and Si-bearing products. The Si concentration ranges from 76 to 217 g/kg in the sulphide-bearing facies. The highest concentrations occur in units 1 and 2 of Core 684, where radiolaria and diatoms are abundant (Fig. 3). The peak of Si, Al, and Na at 1465 cm in Core 683 (Fig. 4) is linked to the presence of basaltic fragments. Elsewhere in the cores, the Si content reflects the hydrothermal clay content. The Mn concentrations in W basin sediments are higher than in those of the SW basin. In Core 684, the highest Mn concentrations are related to the occur-

Table 3. Physical characteristics of the sediments from Core 683 and 684.

	CORE	683			684									
		UNIT L	UNIT U		UNIT 1		UNIT 2	UNIT 3					UNIT 4	UNITS
	SUBUNIT		1100-1180	0-1100	non-met	oxy		3a	3b	3c	3d	3e	3f		2+3+4
1	DSFS (wt%)	57.0	57.0	11.0	45.9	45.9	24.8	15.1	8.3	8.1	10.4	15.5	14.4	6.8	
2	DENSITY (kg/l)	1.85	1.86	1.30	1.71	1.71	1.42	1.32	1.26	1.26	1.28	1.32	1.32	1.25	
3	THICKNESS (cm)	440	80	1100	153	77	155	125	40	85	150	185	80	335	1155
4	MUD MASS (kg/m2)	8180	1450	14320	2620	1320	2200	1650	500	1070	1920	2440	1060	4190	15030
5	DSFS (kg/m2)	4660	827	1575	1200	600	546	250	42	87	200	380	153	285	1943
6	RATE (kg/k.y./m2)			700	109-150										130-162

Notes : Line 1 and 2 : Dry and salt-free sediments (DSFS) and density of the solid fraction are given for each unit and sub-unit. Unit 1 is divided in a non-metalliferous facies (non-met) and a iron-oxyhydroxide facies (oxy). Lines 4 and 5 : mass contained in a column of 1m x 1m x thickness (line 3). Line 6 : mass accumulation rates of the solid fractions for units U, 1 and 2+3+4.

rence of manganese oxyhydroxides. In all samples of Core 683, Mn is present as manganese carbonate. The highest Zn content occurs in the deepest part of each sulphidic facies and decreases upwards. Copper follows similar trends, but shows lower variations than Zn over the sulphide-bearing intervals. Sodium and potassium occur in low concentrations (<13 g/kg). The depth variation of Na and K is similar, and follows approximately that of Si (Figs. 3, 4). Hence, Na and K are assumed to be present in silicate species in detrital material and in authigenic Fe-bearing clays in the metals-rich units. Sodium and potassium are also enriched in the manganese oxyhydroxide-rich sediment. The relation with mineralogy indicates that K is preferably incorporated in todorokite whereas Na is linked to MnO(OH) (groutite and manganite). Except in the Mn-rich facies, the Al concentration shows a pattern similar to that of the alkaline elements. This is because Al is present in the same minerals. In unit 1, the mean concentrations of Zr and Ti of the nonmetalliferous sediments are 0.126 g/kg and 3.21 g/kg, respectively. In the metalliferous units 2, 3, and 4, the mean concentrations are 0.026 g/kg Zr and 0.47 g/kg Ti. Zirconium and titanium are 5 to 7 times less abundant in the metalliferous sediment than in unit 1. The concentrations in Zr and Ti of unit U average 0.018 g/kg and 0.42 g/kg, respectively.

4. DISCUSSION

Based on the high resolution of the mineralogical, chemical, and physical properties of sediments from the Atlantis II Deep, it is possible to discuss the relative importance of the sources that contributed to the mineral deposits in the SW and W basins. The contributions by the various sources over the time span recorded by the stratigraphy can only be defined for elements which were incorporated in the sedimentary solid fraction, after they were supplied to the Atlantis II Deep system. In order to distinguish between soluble and nonsoluble species, the mass of the individual elements contained in the sediment pile is compared with that dissolved in the present-day brine (Fig. 5, Table 4). The calculations use the mean chemical composition of each lithologic unit and consider a column with a cross-section of 1 m^2. The average height of the brine is 71 m (Hartmann, 1980); therefore the sediment contained in a 1 m^2 cross-section is compared with the mass of elements dissolved in 71 m^3 of brine.

The content of alkali metals (Na and K) and alkaline-earth metals (Ca, Mg, and Sr) in the sediment pile is less than what is dissolved in the brine column (Fig. 4), which means that these elements are preferably kept in solution. The alkali and alkaline-earth content of the sediment pile can therefore not be used to define the supply of these elements into the Atlantis II system through time.

The metalliferous sediment in both cores is approximately 200-fold enriched in Si, Fe, and Zn with respect to the present brine (Fig. 4). The enrichment is much greater for Pb, Cu, and Al (>2000) (Fig. 4). Sulphur occurs as both sulphate and sulphide minerals, but reduced sulphur as H_2S has not been detected in the deep brine. Assuming an H_2S concentration of the lower brine equal to the analytical detection limit (e.g., 0.1 μm/l), the enrichment of sulphur in the sediment, relative to the brine, must exceed 20,000.

In the SW basin, where Mn occurs as manganese carbonates, the mass of precipitated Mn is slightly greater than the amount of Mn dissolved in the present brine column. In the W basin, the Mn enrichment is also low in the units in which Mn only occurs as manganese carbonates. For the manganese oxide–bearing units 3a and 3e, Mn is about 10 times enriched with respect to the brine. These low enrichments suggest that the Mn contained in the solid fraction must comprise only a part of the total Mn supplied. Previous studies have shown that Mn^{2+} diffuses out of the lower brine pool into the overlying mixed brine layers (Danielsson et al., 1980; Hartmann, 1985), thus causing precipitation of Mn outside the Atlantis II Deep (Bäcker and Richter, 1973; Bignell et al., 1976).

A chemical mass balance of the metalliferous deposit in the Atlantis II Deep can be achieved for Fe, Si, Al, Zn, Cu, H_2S, Pb, and to a lesser extent for Mn. A chemical mass balance can not be achieved for Na, K, Ca, Mg, and Sr because they have not been immobilized in the sediment.

4.1. The Contribution of Nonmetalliferous Particles

The content of nonmetalliferous particles is very low in the sulphide-rich and oxide-rich units. This is not necessarily an indication of weak contributions from biogenic and detrital sources since dilution and postdepositional dissolution may be important (Anschutz and Blanc, 1993a). If the proportion of nonmetalliferous material is directly proportional to the

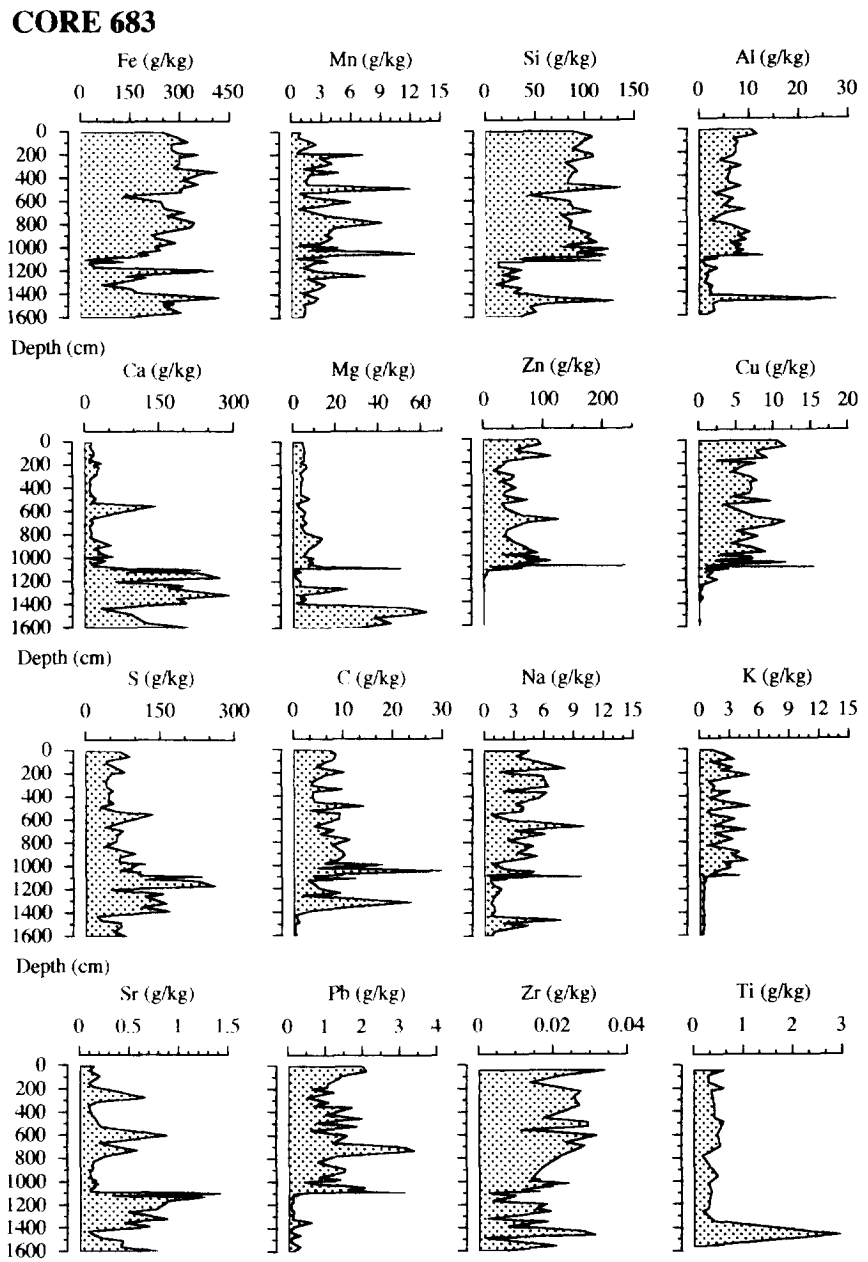

FIG. 3. Concentration vs. depth profiles of chemical components of the dry and salt-free sediment from Core 684.

concentration of a relatively immobile element delivered as detrital particles to the metalliferous sediment, Al, Ti, or Zr could be chosen as indicators of nonmetalliferous contributions. However, Al is mobile in the low-temperature hydrothermal systems (Von Damm et al., 1985, Gamo et al., 1993) and can therefore also be mobile in the Atlantis II Deep system. It is also possible that Al is removed from biogenic silica during early diagenesis (Stoffyn-Egli, 1982). Detection of micromolar concentrations of Al in the present-day lower brine and in the interstitial waters of metalliferous sediments suggest that this may be so (Blanc, 1987). The mean Zr and Ti concentrations are 0.126 g/kg and 3.21 g/kg, respectively, in unit 1, whereas they are about 0.073 g/kg and 1.90 g/kg in the young deep-sea sediment of the Red Sea axial (El Garafi, 1978; Hendricks et al., 1969). Diagenetic reactions involving fish debris probably release Zr into solution (Oudin and Cocherie, 1988). Traces of dissolved Ti have been detected in the interstitial waters of metalliferous sediment from the Atlantis II Deep (Hendricks et al., 1969). Consequently, as Al, Zr, and Ti cannot be considered to be immobile, they cannot be used as indicators of nonmetalliferous sources in the Atlantis II Deep.

A more accurate method to estimate the contribution from the nonmetalliferous source is to calculate a chemical mass balance based on elemental accumulation rates. For this purpose, the age of the Atlantis II sediments must be known. Holocene pelagic sediments from the Red Sea, remote from the deep metalliferous basins, consist of about 50% detrital

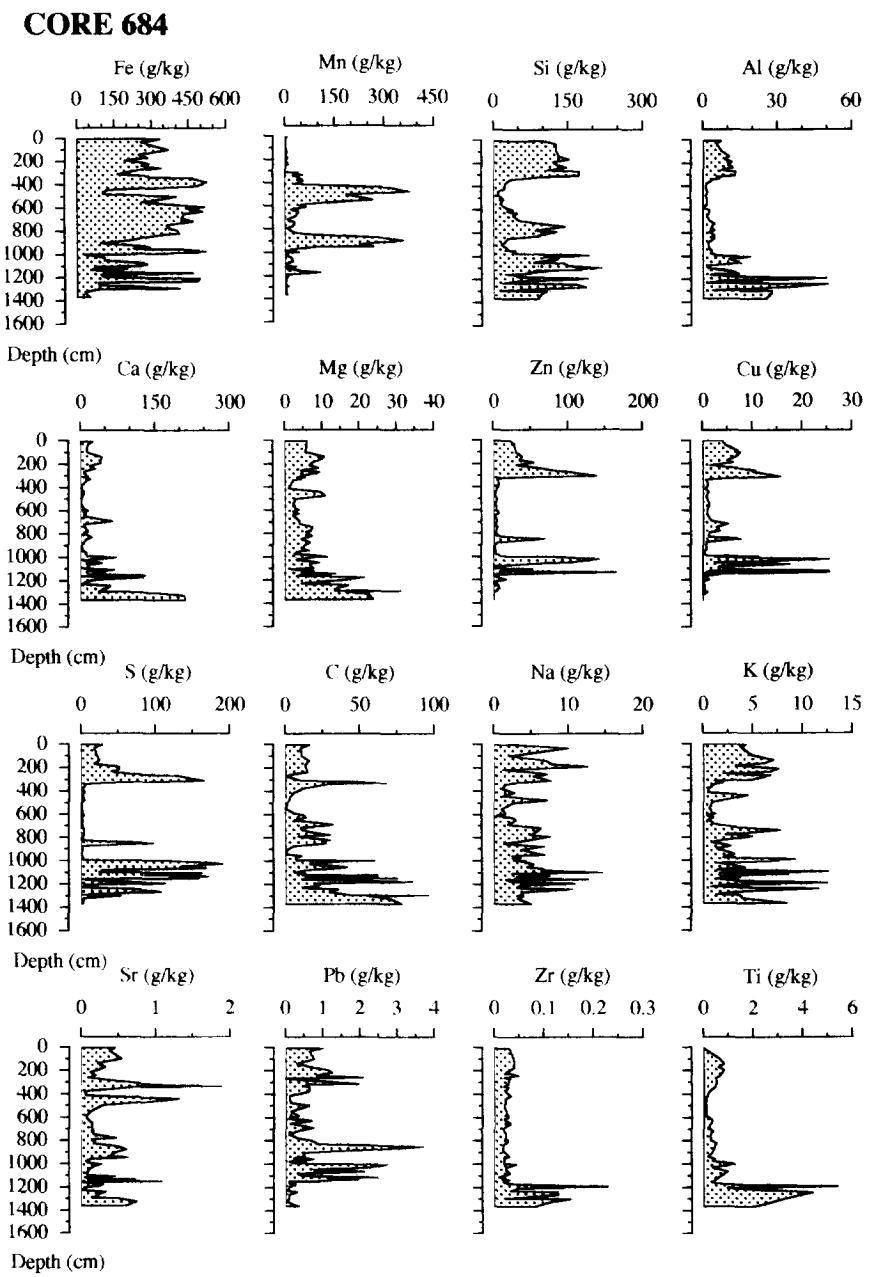

FIG. 4. Concentration vs. depth profiles of chemical components of the dry and salt-free sediment from Core 683.

silicates such as quartz, clay minerals, and volcanic fragments, and 50% carbonaceous tests of foraminifera, pteropods, and other organisms (Bäcker, 1976). Stratigraphic correlations within Red Sea sediments can be obtained by using absolute abundance patterns of planktonic foraminifera. The frequency distribution of planctonic and benthonic foraminifera in cores from the central Red Sea shows that Holocene sediments consist of planktonic foraminiferal zone I (Locke and Thunell, 1988). This zone is characterized by a high total number of planktonic foraminifera, decreasing rapidly downcore to a minimum where the sediment age is close to 11 k.y. Below this, Red Sea cores contain an interval characterized by low abundance or absence of planktonic foraminifera and relative high abundance of pteropods (Berggren and Boersma, 1969; Reiss et al., 1980). The base of this "aplanktonic zone" occurs around 20 k.y. BP (Reiss et al., 1980). Core 684 contains a similar "aplanktonic" interval located between 1340 cm in unit 1 and somewhere in unit 2 (Anschutz and Blanc, 1993a). Assuming that the sedimentation rate was constant during the deposition of unit 1, and excluding the oxyhydroxide layers of this unit, the remaining 155 cm of nonmetalliferous sediments of Core 684 could have been deposited between 23 and 11 k.y. BP at the latest. The ^{14}C datation of sediments from the Atlantis II Deep indicates that the age of the oldest sediment is between 20 and 25 k.y. BP, and that the purely nonmetalliferous sedimentation (unit 1) ended be-

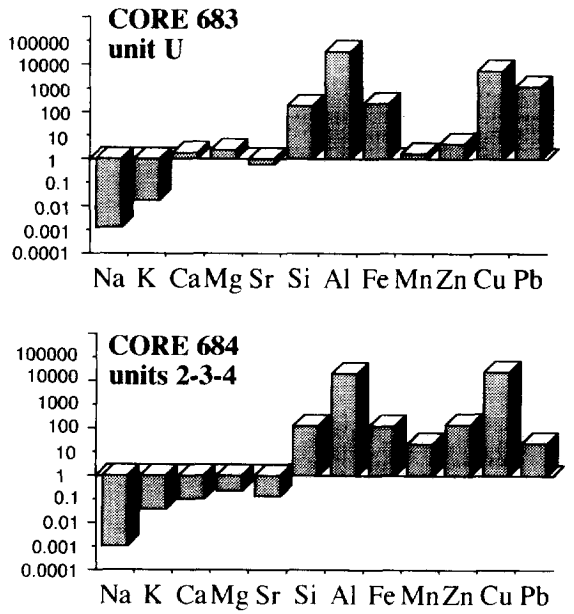

FIG. 5. Ratios of the elementary masses contained in the sedimentary pile of unit U (Core 683) and of units 2, 3 and 4 (Core 684) vs. those dissolved in a 71 m column of the present-day brine. The species which are more abundant in the present-day brine show values below unity. The species with ratios $\gg 1$, have been preferentially immobilized in the sedimentary pile.

tween 12 and 15 k.y. ago (Ku et al., 1969; Hackett and Bischoff, 1973; Shanks and Bischoff, 1980). Our estimates agree with this. Thus, the deposition of nonmetalliferous unit 1 of Core 684 may have occurred over a period of 8 to 11 k.y. (i.e., between 23 and 15–12 k.y. BP). We can therefore assume a sedimentation rate of 14 to 20 cm/k.y. for the nonmetalliferous particles in unit 1. For a 1 m^2 cross-section we calculate a mass accumulation rate of 109–150 kg/k.y./m^2 for the nonmetalliferous particles in unit 1 (Table 3). Tjis give a sedimentation rate of 1155 cm/12–15 k.y. (77–97 cm/k.y.) and a mass accumulation rate of 1943 kg/12–15 k.y./m^2 (130–162 kg/k.y./m^2) for the total solid fraction of units 2, 3, and 4 (Table 3). Absolute dating of Pleistocene-Holocene Red Sea sediments (Ku et al., 1969; Milliman et al., 1969; Reiss et al., 1980; Locke and Thunell, 1988) range between 2 and 18 cm/k.y. depending of the location of the core within the Red Sea basin. The relatively constant sedimentation rates in these cores over the last 25 k.y. is a specific feature of the Red Sea; the sedimentation rate in the world oceans shows much greater variations during the same period. The chemical composition of biogenic and detrital sediments of the Red Sea varied little across the Pleistocene-Holocene boundary (Locke and Thunell, 1988). Thus, the sedimentation rate of nonmetalliferous sediments during the deposition of units 2, 3, and 4 was similar to that of unit 1, i.e. 109–150 kg/k.y./m^2. The accumulation rate of the nonmetalliferous sediments in the W basin of the Atlantis II Deep was thus approximately the same as the sedimentation rate of the metalliferous sediments (130–162 kg/k.y./m^2). This is unexpected, because units 2, 3, and 4 of the Core 684 contain mostly metalliferous particles, whereas biogenic calcite and detrital silicates often comprise less than 10%. Consequently, the major part of nonmetalliferous particles dissolved during or after deposition in the Atlantis II Deep.

Microbiostratigraphic correlations between Cores 684 and 683 show that the sulphide-rich part of unit U of Core 683 (from 1,100 cm to the top) was deposited during the same period as unit 4 of Core 684 (Anschutz and Blanc, 1993a). Unit 4 corresponds to 15% of the mass of metalliferous sediments of Core 684. Assuming a constant average accumulation rate for the metalliferous sediments of the W basin, the age of the base of unit 4 could not exceed 2,250 years (i.e., 15,000 × 0.15). A cross-section of 1 m^2 of unit U contains 1,575 kg of sediment (Table 3). Therefore, the mass accumulation rate of unit U is 700 kg/k.y./m^2. The proportion of biogenic material settling during a 2.25 k.y. period might be 245 to 340 kg and account for 15 to 22% of the unit U sedimentary pile. Biogenic tests are very sparse in this unit (less than 1%) and detritus was not observed. Therefore, the biogenic and detrital inputs acted as source of chemical components to the metalliferous sediments through their dissolution. Silicon amounts to 12% of the detrital facies in unit 1 and the Holocene Red Sea pelagic sediments (Bischoff, 1969). But 12% of an accumulation rate of 109–150 kg/k.y./m^2 represents a minimum accumulation rate for detrital Si of 109 kg/k.y./m^2 × 0.12 × 12 k.y. ≈ 150 kg/m^2 during the deposition of units 2, 3, and 4, and 109 kg/k.y./m^2 × 0.12 × 2.25 k.y. ≈ 30 kg/m^2 during the deposition of unit U. Such an accumulation rate is large enough to account for the entire mass of Si in units 2, 3 and 4, and 20% of the Si content of unit U. Because Si contained in metalliferous sediments mainly occurs as authigenic iron silicates, our calculation suggests that Si derived from nonmetalliferous particles must contribute to the formation of authigenic silicates beyond the hydrothermal Si input. Conversely, calculations using Fe, Mn, Zn, Cu, and Pb indicate that the biogenic and detrital inputs did not contribute much to the metal content of the metalliferous sediments, with the exception of Pb. Lead accounts for 175 ppm of the biogenic and detrital facies of unit 1, whereas a maximum Pb content of 360 ppm was measured for foraminifera (Turekian, 1965). Considering an accumulation rate of 109–150 kg/k.y./m^2, 175 ppm give a minimum biogenic Pb accumulation of 230 g/m^2 during the deposition of units 2, 3, and 4 and 43 g/m^2 during the deposition of unit U. This nonhydrothermal Pb contributes to more than 14% of total Pb in the units 2, 3, and 4, and 2% in unit U. Core 684 is enriched in diatoms in units 2 and 3b (Anschutz and Blanc, 1993a) where they represent between 5 and 10% of the mass of sediments. Diatom frustules average 3300 ppm Pb (Hurd, 1973) which can account for more than 20% of the Pb contained in these units. Unit 3a is also enriched in Pb, which likely comes from the dissolution of diatom frustules. These results agree with measurements of the lead isotopic compositions of Cores 683 and 684, which indicate that the nonmetalliferous endmember is important for Pb (Dupré et al., 1988). The present study shows that a part of the Pb contained in the metalliferous sediments originated from the Holocene biogenic sedimentation via diagenetic reactions.

Table 4. Concentration of dissolved species in Red Sea deep water (H2) and in the lower brine of the Atlantis II Deep (H6) in 1985 (data from Blanc, 1987).

	Na Mol/l	K Mol/l	Ca Mol/l	Mg Mol/l	Sr mMol/l	Rb μMol/l	Mn mMol/l	Zn μMol/l	Cu nMol/l	Fe mMol/l
H2	0.548	0.0114	0.011	0.0584	0.137	1.54	<	<	<	<
H6	4.86	0.059	0.138	0.0292	0.684	23.9	1.77	81.1	80	1.17

	Pb nMol/l	Cd nMol/l	Cl Mol/l	SO_4 mMol/l	HCO_3 mMol/l	B mMol/l	Si μMol/l	Al μMol/l	pH
H2	<	<	0.645	33.9	2.31	0.481	6.78	<	8.22
H6	45.9	508	5.37	8.89	0.833	0.849	584	0.294	5.8

4.2. The Contribution of Mineralizing Fluid to Ore-Forming Elements

The content of ore-forming elements in the sediment offers the possibility to estimate the chemical composition and the flux of element via the inflowing hydrothermal brines. In the Atlantis II Deep, the metalliferous sediments show high concentrations of ore-forming elements (Fe, Mn, Zn, Cu, Pb, and reduced S) which originated with the flowing hydrothermal solution. Because iron is ubiquitous, abundant, and mostly of hydrothermal origin in all the metalliferous facies of Cores 683 and 684, the Me/Fe molar ratios (Me being Mn, Zn, Cu, Pb, or S) of the solid fraction is assumed to be similar to those in the hydrothermal fluids from which these elements precipitated (Fig. 6). For reduced S, the Me/Fe ratio is expressed as the H_2S/Fe ratio of the dissolved species. The Me/Fe ratios obtained compare favorably with those of the most Fe-rich geothermal brine from Salton Sea and the black smoker hydrothermal fluids from Southern Juan de Fuca ridge (SJdF) (Fig. 6). Iron concentrations in the fluids from Salton Sea and SJdF are 36.2 mmol/L and 18.7 mmol/L (Williams and McKibben, 1989; Von Damm and Bischoff, 1987). Assuming that the dissolved Fe concentration in the inflowing hydrothermal fluids to the Atlantis II Deep is in the same range than those of Salton Sea and SJdF, we calculate that 280–560 m^3 of such fluids are required to supply the 566 kg of Fe contained in the 1 × 1 × 11.55 m box of units 2, 3, and 4 of Core 684. These volumes are 4 to 8 times the average volume of the overlying brine column (i.e., 71 m^3). A fourfold to eightfold renewal rate of the present-day lower brine pool (3.1×10^9 m^3; Hartmann, 1980) during the last 12–15 k.y. corresponds to an average inflow of $1-2 \times 10^9$ m^3/k.y. (i.e., from 30 to 60 L/s) which is substantially less than, but nonetheless somewhat comparable to the estimated local flow of 150 ± 60 L/s for the EPR 21°N black smockers field (Converse et al., 1984).

In the metalliferous units 2, 3, 4, and U from Cores 684 and 683, the Me/Fe ratios show great variations (Fig. 6). These variations can be used to define changes in the physical and chemical parameters which lead to the accumulation of the ore forming elements through the time.

4.2.1. Units 2, 4, and U

Microbiological and chemical investigations strongly suggest that the sulphide-rich unit U of Core 683 (from 11,000

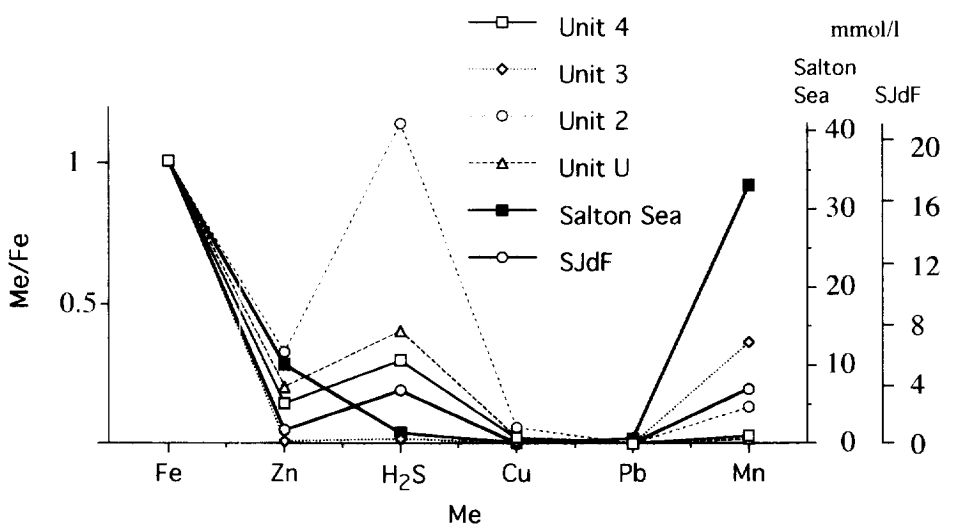

FIG. 6. Diagram showing the Me/Fe molar ratios (Me being Zn, Cu, Pb, Mn, H2S) of the metalliferous sediments. H_2S represents reduced forms of sulfur contained in sulfide minerals. Assuming that the values of these Me/Fe molar ratios are equal to those of inflowing fluids from which these elements precipitated, they are compared to those of Salton Sea brine and South Juan de Fuca Plume hydrothermal solution. The metal concentrations for Salton Sea and SJdF solutions (in millimoles per liter) given by Williams and McKibben (1989), and Von Damm and Bischoff (1987) are reported in the scale bars on the right side of the diagram.

cm to the top) was deposited during the same time as unit 4 of Core 684 (Anschutz and Blanc, 1993a). However, the Zn/Fe, Cu/Fe, and H_2S/Fe ratios of unit U are higher and the Mn/Fe ratio is lower than those of unit 4. Because sulphide minerals, mostly sphalerite and chalcopyrite, are deposited preferably near the mineralizing fluid source, and because Mn is more mobile than other metals, the fluid source was likely located in, or near, the SW basin during the deposition of these units. The Zn/Fe ratios of the sulphide facies (units 2, 4, and U) are similar to that of Salton Sea fluid. In unit 2, the Zn/Fe ratio equal 0.32, and the H_2S/Fe ratio reaches a high value of 1.13. This indicates that during the ZnS deposition period, the deep was recharged either by a more concentrated solution than Salton Sea, or by a greater volume of less metal-enriched brine, i.e., a discharge flow greater than 30 L/s. The first assumption implies a hotter or more acidic solution allowing more Zn and more H_2S to be transported together (Barrett and Anderson, 1988). The second assumption is supported by the fact that the brine pool volume was at least twice as great as the present-one during the period of deposition of unit 2 (Bäcker and Richter, 1973). For the youngest units 4 and U, the H_2S/Fe ratios are significantly higher than the ratio in Salton Sea. Therefore, the same explanation as that proposed for unit 2 can be invoked for the recent brine inputs. The Cu/Fe ratio of sulphide-bearing units 2, 4, and U show values of 0.056, 0.020, and 0.023, respectively. These values are much greater than the Cu/Fe ratios in the of Salton Sea (0.002) or SJdF (<0.0002), and suggest that the mineralizing fluid was hot, acidic, or supplied in abundance during the periods of deposition. Chalcopyrite is the main Cu-bearing mineral. Most of the sulphides occur as less than 2 μm grains in the Atlantis II Deep stratiform sediment. However, there are also rounded and fissured chalcopyrite particles up to 35 μm in size (Pottorf and Barnes, 1983). This suggests mechanical transport of previously precipitated particles, which can explain the high Cu/Fe ratios in the sediment. The Pb/Fe ratios in units 2, 4, and U are intermediate between those of Salton Sea and SJdF. The high Pb content of the Salton Sea solution is typical of continental geothermal systems, and the low Pb content of SJdF is typical of oceanic hydrothermalism (White, 1981). Intermediate values of Pb/Fe of metalliferous sediment of the Atlantis II Deep suggest another source of Pb than basaltic crust, as noted by Dupré et al. (1988). Mn/Fe ratios of sulphide-bearing units are lower than Mn/Fe ratio of Salton Sea and SJdF. However, the Mn contained in the solid fraction must comprise only a part of the supplied Mn, and the Mn/Fe ratio must be under estimated.

4.2.2. Unit 3

With the exception of Mn, the Me/Fe ratios in unit 3 are low (Fig. 6). Because manganese oxides are soluble in reducing solutions (Stumm and Morgan, 1981), the conservation of manganese oxides within the subunits 3a and 3e could be related to the occurrence of an oxidizing environment during this period of deposition. In such an environment Zn, Cu, and H_2S are insoluble and could not be carried from the discharge zone (i.e., SW basin) into the W basin. This may explain the low Zn/Fe, Cu/Fe, and H_2S/Fe ratios in unit 3. However, the great amount of Fe-bearing minerals within unit 3 sediments strongly suggests that the W basin was filled by a reducing brine during the corresponding deposition periods. Indeed, dissolved Fe can not be carried in an oxidizing environment, whereas iron oxides can persist in a reducing environment, such as in the deep today (Bischoff, 1969; Badaut, 1988). Furthermore, manganosiderite, which is stable in contact with reducing solutions, occurs in iron-oxide–rich subunits (Fig. 3). Hence, the low concentrations in Zn, Cu, and H_2S of unit 3 a, c, d, e, and f did probably not result from changes in redox conditions. More likely, the incoming fluids that supplied the deep during these periods of deposition were depleted in Zn, Cu, and H_2S, and only enriched in Fe and Mn. Sulphide minerals become insoluble when the temperature decreases (Barnes, 1979). During the period of the unit 3 deposition, the hot-spring fluids had probably lost heat on ascending to the seafloor, and the major part of dissolved Zn, Cu, and H_2S had precipitated within the internal plumbing of the Atlantis II Deep, before the mineralizing fluids reached the point of discharge.

5. CONCLUSION

Cores 683 and 684 contain all the lithologic facies which have been described in the several hundred cores collected previously in the Atlantis II Deep. High resolution sampling and chemical, mineralogical, and biostratigraphic data allow mass accumulation rates to be calculated for all lithological units and a geochemical mass balance to be constructed for the Atlantis II Deep hydrothermal system.

The metalliferous and nonmetalliferous sediments in the W basin accumulated at similar rates, averaging 150 kg/k.y./m^2. This indicates that the chemical components of the biogenic and detrital particles mostly dissolved and subsequently became incorporated into authigenic minerals. The metalliferous sediments from the SW basin accumulated at the same time as the youngest lithologic unit of the W basin, at a rate of about 700 kg/k.y./m^2.

The chemical mass balance of metalliferous sediments strongly suggests that the discharge points of the inflowing mineralizing brines were located in, or near, the SW basin during the last 2.25 k.y. Because Fe, Mn, Zn, Cu, Pb, and S are highly enriched in the solid fractions relative to the present-day hydrothermal brine, they can be considered to have been insoluble over the entire hydrothermal history of the deep. Ore forming elements such as Fe, Mn, Zn, Cu, and S were supplied mostly by a hot hydrothermal brine, whereas biogenic sedimentation acted as an additional source of Pb. The (S + Cu + Zn)/Fe ratios in the oxide-rich facies are lower than in the sulphide-rich facies. The difference is probably more due to changes in the chemical composition of the inflowing mineralizing fluids rather than to changes in the redox conditions of the brine pool. Assuming Fe concentrations in the inflowing Atlantis II brines equal to those of Salton Sea or Southern Juan de Fuca, the chemical mass balance indicates that the volume of fluid which supplied the Deep during the Atlantis II hydrothermal history should have been at least four times the volume of the present-day brine pool. For a Salton Sea-like solution, 30 L/s is the minimum discharge flow to supply all the Fe that has accumulated in the metalliferous sediments of the W basin during 12–15 k.y. BP.

Acknowledgments—The authors are very grateful to G. Krempp, J. L. Cézard, R. Wendling, J. Samuel, R. Rouault, and J. Balouka (Centre de Géochimie de la Surface, CNRS) and the marine staff of the R/V *Marion Dufresne* for technical assistance. We thank Dr. R. W. Murray and two anonymous reviewers for comprehensive comments and constructive suggestions. We also wish to thank Dr. W. Ullmann and Dr B. Sundby who greatly improved English. This study was sustained by a Ph.D. grant from the government of France, and the Marine Geosciences Committee of the INSU-CNRS.

Editorial handling: M. A. McKibben

REFERENCES

Anschutz P. (1993) Genèse et évolution géochimique des sédiments métallifères de la fosse Atlantis II (mer Rouge). Ph.D. dissertation, Univ. Louis Pasteur.

Anschutz P. and Blanc G. (1993a) L'histoire sédimentologique de la fosse Atlantis II (mer Rouge). Les apports de la micropaléontologie. *C. R. Acad. Sci., Paris*, série II **317,** 1303–1308.

Anschutz P. and Blanc G. (1993b) Le rapport NaCl/eau des boues minéralisées de la fosse Atlantis II (mer Rouge). Calcul de la teneur en halite des sédiments et implication sur la paléotempérature de milieu. *C. R. Acad. Sci., Paris*, série II **317,** 1595–1600.

Anschutz P. and Blanc G. (1995) Geochemical dynamics of the Atlantis II Deep (Red Sea): Silica behavior. *Mar. Geol.* (in press).

Bäcker H. (1976) Facies und chemische Zusammensetzung rezenter Ausfäblungen aus Mineralquellen im Roten Meer. *Geol. Jahrb.* **D17,** 151–172.

Bäcker H. and Richter H. (1973) Die rezente hydrothermal-sedimentäre Lagestätte Atlantis II Tief im Roten Meer. *Geol. Rundsch.* **62,** 697–741.

Bäcker H. and Schoell M. (1972) New deeps with brines and metalliferous sediments in the Red Sea. *Nature Phys. Sci.* **240,** 153–158.

Badaut D. (1988) Les argiles et les composés silico-ferriques des sediments metallifères de la fosse Atlantis II (Mer Rouge). Formation et diagenèse des dépôts. Ph.D. dissertation, Univ. Paris Sud.

Badaut D., Blanc G., and Decarreau A. (1990) Variation des minéraux argileux ferrifères, en fonction du temps et de l'espace, dans les dépots métallifères de la fosse Atlantis II en Mer Rouge. *C. R. Acad. Sci., Paris*, série II **310,** 1069–1075.

Barnes H. L. (1979) Solubilities of ore minerals. In *Geochemistry of Hydrothermal Ore Deposits* (ed. H. L. Barnes), pp. 404–460. Wiley.

Barrett T. J. and Anderson G. M. (1988) The solubility of sphalerite and galena in 1–5 m NaCl solutions to 300°C. *Geochim. Cosmochim. Acta* **52,** 813–820.

Berggren W. A. and Boersma A. (1969) Late Pleistocene and Holocene planktonic foraminifera from the Red Sea. In *Hot Brines and Recent Heavy Metal Deposits in the Red Sea* (ed. E. T. Degens and A. D. Ross), pp. 282–298. Springer-Verlag.

Bignell R., Cronan D., and Tooms J. (1976) Metal dispersion in the Red Sea as an aid to marine geochemical exploration. *Inst. Mining Metall. Trans.* **84,** B274–B278.

Bischoff J. L. (1969) Red Sea geothermal brine deposits: Their mineralogy, chemistry, and genesis. In *Hot Brines and Recent Heavy Metal Deposits in the Red Sea* (ed. E. T. Degens and A. D. Ross), pp. 368–401. Springer-Verlag.

Blanc G. (1987) Géochimie de la fosse Atlantis II (Mer Rouge). Evolution spatio-temporelle et rôle de l'hydrothermalisme. Ph.D. dissertation, Univ. Pierre et Marie Curie Paris VI.

Blanc G. and Anschutz P. (1995) New hydrographic situation in the Atlantis II Deep hydrothermal brine system. *Geology* **23,** 543–546.

Blanc G., Boulègue J., Badaut D., and Stouff P. (1986) Premiers résultats de la campagne océanographique Hydrotherm (mai 1985) du Marion-Dufresne sur la fosse Atlantis II (Mer Rouge). *C. R. Acad. Sci., Paris*, série II **302,** 175–180.

Blanc G., Boulègue J., and Charlou J. L. (1990) Profils d'hydrocarbures légers dans l'eau de mer, les saumures et les eaux interstitielles de la fosse Atlantis II (mer Rouge). *Oceanologica Acta* **13,** 187–198.

Brockamp O., Goulard E., Harder H., and Heydemann A. (1978) Amorphous Copper and Zinc sulfides in the metalliferous sediments of the Red Sea. *Contrib. Mineral. Petrol.* **68,** 85–88.

Converse D. R., Holland H. D., and Edmond J. M. (1984) Flow rates in the axial hot springs of the East Pacific Rise (21°N): Implication of massive sulfide deposits. *Earth Planet. Sci. Lett.* **69,** 159–175.

Danielsson L. G., Dyrssen D., and Graneli A. (1980) Chemical investigations of Atlantis II and Discovery brines in the Red Sea. *Geochim. Cosmochim. Acta* **44,** 2051–2065.

Degens E. T. and Ross D. A. (1969) *Hot Brines and Recent Heavy Metal Deposits in the Red Sea.* Springer-Verlag.

Dupré B., Blanc G., Boulègue J., and Allègre C. J. (1988) Metal remobilization at a spreading centre studied using lead isotopes. *Nature* **333,** 165–167.

El Garafi A. (1978) Geochemie und sedimentfazies des Port Sudan Tief-Rotes Meer-Sudan. Ph.D. dissertation, Univ. Hamburg.

Gamo T. et al. (1993) Hydrothermal plumes in the eastern Manus Basin, Bismarck Sea: CH_4, Mn, Al and pH anomalies. *Deep-Sea Res.* **40,** 2335–2349.

Goldsmith J. R. and Graf D. L. (1958) Relation between lattice constants and composition of the Ca-Mg carbonates. *Amer. Mineral.* **43,** 84–101.

Hackett J. and Bischoff J. L. (1973) New data on the stratigraphy, extent, and geologic history of the Red Sea geothermal deposits. *Econ. Geol.* **68,** 553–564.

Hartmann M. (1980) Atlantis II deep geothermal brine system. Hydrographic situation in 1977 and changes since 1965. *Deep-Sea Res.* **27A,** 161–171.

Hartmann M. (1985) Atlantis II deep geothermal brine system. Chemical processes between hydrothermal brines and Red Sea deep water. *Mar. Geol.* **64,** 157–177.

Hendricks R. L., Reisbick F. B., Mathaffey E. J., Roberts D. B., and Peterson M. N. A. (1969) Chemical composition of sediments and interstitial brines from the Atlantis II, Discovery and Chain deeps. In *Hot Brines and Recent Heavy Metal Deposits in the Red Sea* (ed. E. T. Degens and A. D. Ross), pp. 407–440. Springer-Verlag.

Hooton D. H. and Giorgetta N. A. (1977) Quantitative X-Ray diffraction analysis by a direct calculation method. *X-Ray Spectrometry* **6,** 2–5.

Hurd D. C. (1973) Interaction of biogenic opal, sediment and seawater in the central Equatorial Pacific. *Geochim. Cosmochim. Acta* **37,** 2257–2282.

Ku T. L., Thurber D. L., and Mathieu G. G. (1969) Radiocarbon chronology of Red sea sediments. In *Hot Brines and Recent Heavy Metal Deposits in the Red Sea* (ed. E. T. Degens and A. D. Ross), pp. 348–359. Springer-Verlag.

Locke S. and Thunell R. C. (1988) Paleaceanographic record of the last glacial/interglacial cycle in the Red Sea and Gulf of Aden. *Palaeogeogr. Palaeoclimatol. Palaeoecol.* **64,** 163–187.

Miller A. R. et al. (1966) Hot brines and recent iron deposits in deeps of the Red Sea. *Geochim. Cosmochim. Acta* **30,** 341–359.

Milliman J. D., Ross D. A., and Ku T. L. (1969) Precipitation and lithification of deep-sae carbonates in the Red Sea. *J. Sediment. Petrol.* **39,** 724–736.

Missack E., Stoffers P., and El Goresy A. (1989) Mineralogy, paragenesis, and phases relations of copper iron sulfides in the Atlantis II deep, Red Sea. *Mineral. Deposita* **24,** 82–91.

Oudin E. and Cocherie A. (1988) Fish debris record the hydrothermal activity in the Atlantis II Deep sediments (Red Sea). *Geochim. Cosmochim. Acta* **52,** 177–184.

Pautot G. (1983) Les fosses de la Mer Rouge: Approche géomorphologique d'un stade initial d'ouverture océanique réalisée à l'aide du Seabeam. *Oceanol. Acta* **6,** 235–244.

Pottorf R. J. and Barnes H. L. (1983) Mineralogy, geochemistry, and ore genesis of hydrothermal sediments from Atlantis II deep, Red Sea. *Econ. Geol. Monogr.* **5,** 198–223.

Ramboz C. and Danis M. (1989) Superheating in the Red Sea? The heat-mass balance of the Atlantis II Deep revisited. *Earth Planet. Sci. Lett.* **97,** 190–210.

Reiss Z., Luz B., Almogi-Labin A., Halicz E., Winter A., Wolf M., and Ross D. A. (1980) Late quaternary paleoceanography of the Gulf of Aqaba (Elat), Red Sea. *Quat. Res.* **14,** 294–308.

Samuel J., Rouault R., and Besnus Y. (1985) Analyse multiélémentaire standardisée des matériaux géologiques en spectrométrie d'émission par plasma à couplage inductif. *Analusis* **13,** 312–317.

Schoell M. (1975) Heating and convection within the Atlantis II Deep geothermal system of the Red Sea. *Proceed. Scd. Unit. Nat. Symp. on the Development and Use of Geothermal Resources* **2,** 583–590.

Schoell M. and Hartmann M. (1973) Detailed temperature structure of the hot brines in the Atlantis II Deep area (Red Sea). *Mar. Geol.* **14,** 1–14.

Schoell M. and Hartmann M. (1978) Changing hydrothermal activity in the Atlantis II Deep geothermal system. *Nature* **274,** 784–785.

Shanks W. L., III and Bischoff J. L. (1977) Ore transport and deposition in the Red sea geothermal system: a geochemical model. *Geochim. Cosmochim. Acta* **41,** 1507–1519.

Shanks W. L., III and Bischoff J. L. (1980) Geochemistry, sulfur isotope composition and accumulation rates of the Red Sea geothermal deposits. *Econ. Geol.* **75,** 445–459.

Stiers W. and Schwertmann U. (1985) Evidence for manganese substitution in synthetic goethite. *Geochim. Cosmochim. Acta* **49,** 1909–1911.

Stoffyn-Egli P. (1982) Dissolved aluminium in interstitial waters of recent terrigenous marine sediments from the North Atlantic Ocean. *Geochim. Cosmochim. Acta* **46,** 1345–1352.

Stumm W. and Morgan J. J. (1981) *Aquatic Chemistry,* 2nd ed. Wiley.

Thisse Y. (1982) Sédiments métallifères de la fosse Atlantis II (Mer Rouge). Contribution à l'étude de leur contexte morphostructural et de leurs caractéristiques minéralogiques et géochimiques. Ph.D. dissertation, Univ. Orléans.

Turekian K. K. (1965) Some aspects of the geochemistry of marine sediments. In *Chemical Oceanography* (ed. J. P. Riley and G. Skirrow), pp. 81–126. Academic Press.

Turner J. S. (1969) A physical interpretation of the observations of the hot brine layers in the Red Sea. In *Hot Brines and Recent Heavy Metal Deposits in the Red Sea* (ed. E. T. Degens and A. D. Ross), pp. 164–173. Springer-Verlag.

Urvois M. (1988) Apports de l'estimation géostatistique de l'épaisseur des unités métallifères dans la compréhension des mécanismes de mise en place des sédiments de la fosse Atlantis II (Mer Rouge). *Doc. BRGM. 154.*

Von Damm K. L. and Bischoff J. L. (1987) Chemistry of hydrothermal solutions from the Southern Juan de Fuca Ridge. *J. Geophys. Res.* **92,** 11,334–11,346.

Von Damm K. L., Edmond J. M., Grant B., Measures C. I., and Weiss R. F. (1985) Chemistry of submarine hydrothermal solutions at 21°N, East Pacific Rise. *Geochim. Cosmochim. Acta* **49,** 2197–2220.

Voorhis A. D. and Dorson D. L. (1975) Thermal convection in the Atlantis II hot brine pool. *Deep-Sea Res.* **22,** 167–175.

White D. E. (1981) Active geothermal systems and hydrothermal ore deposits. *Econ. Geol* (75th Anniversary Vol.), pp. 392–423.

Williams A. E. and McKibben M. A. (1989) A brine interface in the Salton Sea geothermal system, California: Fluid geochemical and isotopic characteristics. *Geochim. Cosmochim. Acta* **53,** 1905–1920.

Zhabina N. N. and Solokov V. S. (1982) Sulphur compounds in the sediments of the Atlantis II deep, Red Sea. *Mar. Geol.* **50,** 129–142.

Zierenberg R. A. and Shanks W. C., III (1983) Mineralogy and geochemistry of epigenetic features in metalliferous sediments, Atlantis II Deep, Red Sea. *Econ. Geol.* **78,** 57–72.

Zierenberg R. A. and Shanks W. C., III (1988) Isotopic studies of epigenetic features in metalliferous sediments, Atlantis II deep, Red Sea. *Canadian Mineral.* **26,** 737–753.